

Extrasolar Trojans: The Viability and Detectability of Planets in the 1:1 Resonance

Gregory Laughlin¹, John E. Chambers²

¹ UCO/Lick Observatory, UCSC, Santa Cruz, CA 95064 laugh@ucolick.org

² NASA Ames Research Center, Moffett Field, CA 94035 john@mycenae.arc.nasa.gov

Received _____; accepted _____

ABSTRACT

We explore the possibility that extrasolar planets might be found in the 1:1 mean-motion resonance, in which a pair of planets share a time-averaged orbital period. There are a variety of stable co-orbital configurations, and we specifically examine three different versions of the 1:1 resonance. In the first configuration, the two planets and the star participate in tadpole-type librations about the vertices of an equilateral triangle. The dynamics of this situation resemble the orbits of Jupiter’s Trojan asteroids. We show analytically that an equilateral configuration consisting of a star and two equal-mass planets is linearly stable for mass ratios $\mu = 2m_{pl}/(2m_{pl} + M_\star) < 0.03812$. When the equilateral configuration is subjected to larger perturbations, a related 1:1 resonance occurs. In this second family of configurations, the planet pair executes horseshoe-type orbits in which the librating motion in the co-rotating frame is symmetric about a 180° separation. The Saturnian satellites Janus and Epimetheus provide a solar system example of this phenomena. In the case of equal mass planets, a numerical survey indicates that horseshoe configurations are stable over long periods for mass ratios $\mu < 0.0004$, indicating that a pair of Saturn-mass planets can exist in this resonance. The third configuration which we examine is more exotic, and involves a pair of planets which exchange angular momentum in a manner that allows them to indefinitely avoid close encounters. An illustrative example of this resonance occurs when one planet has a highly eccentric orbit while the other planet moves on a nearly circular orbit; the periapses are in alignment, and conjunctions occur near periapse. All three of these resonant configurations can be stable over timescales comparable to or longer than stellar lifetimes. We show that pairs of planets in 1:1 resonance yield characteristic radial velocity signatures which are not prone to the $\sin(i)$ degeneracy. Indeed, Keplerian fits to the

radial velocities cannot reveal the presence of two planets in the 1:1 resonance. We discuss a dynamical fitting method for such systems, and illustrate its use with a simulated data set. Finally, we argue that hydrodynamical simulations and torqued three-body simulations indicate that 1:1 resonant pairs might readily form and migrate within protostellar disks.

Subject headings: stars: planetary systems

1. Introduction

In 1772, Lagrange proved the existence of five equilibrium points in the equilateral three-body problem (Lagrange 1867-1892). A century later, in 1875, Routh described the librating motion of a particle in the vicinity of the triangular equilibrium points L_4 , and L_5 (e.g. Routh 1898). Near the turn of the last century, in 1906, Max Wolf of the Heidelberg observatory discovered the first Trojan asteroid, 588 Achilles. This object is participating in stable librations about Jupiter’s L_4 point. The extent of the Jovian Trojan population is now thought to rival the main asteroid belt (Shoemaker, Shoemaker, & Wolfe 1989).

Several thousand nearby stars are now being surveyed for periodic radial velocity variations which indicate the presence of extrasolar planets (Marcy, Cochran & Mayor 2000). Systems with more than one planet are starting to emerge from the surveys, and among these multiple-planet systems there are already interesting examples of resonant relationships. For example, the planetary system orbiting ν Andromedae displays a secular resonance in which the arguments of periastron of the outer two planets librate about an aligned configuration (Chiang, Trembachnik & Tremaine 2001), and the pair of planets orbiting GJ 876 are clearly participating in the 2:1 resonance (Marcy et al 2001, Laughlin & Chambers 2001, Lee & Peale 2001).

Given that resonances are likely to be very common among extrasolar planets, one can ask whether it is possible to have co-orbital planets, both with masses of the order of Jupiter. In this paper, we argue that such “trojan planets” are indeed a viable possibility. Configurations of this type are stable over a fairly wide and varied range of orbital parameters. Furthermore, a 1:1 resonance between a pair of extrasolar planets induces a characteristic radial velocity signature in the parent star. Such a signature may already exist unrecognized in the radial velocity data set, as the identification of a 1:1 resonance requires a self-consistent dynamical fitting procedure.

This paper is organized as follows. In the next section (§2), we describe the dynamics of three flavors of 1:1 resonance. In §3 we show how self-consistent fits to the radial velocities induced by co-orbital planets are derived. In §4 we conclude with a discussion of how co-orbital planets might form.

2. The Dynamics of the 1:1 resonance

It is well known that an equilateral triangle configuration represents an equilibrium point in the restricted 3-body problem in which one of the bodies has a negligible mass. The configuration is stable to small perturbations provided that the smaller of the two massive bodies has a mass less than $0.03852\dots$ in units of the total mass (*e.g.* Murray and Dermott 1999). Here we examine the stability of the equilateral triangle configuration in the general 3-body problem.

Consider 3 spherical bodies with masses m_0 , m_1 and m_2 , such that $m_1, m_2 \leq m_0$, confined to move in a plane. In a coordinate system centered on m_0 , the acceleration on body m_1 is given by

$$\ddot{\mathbf{r}}_1 = -\frac{G(m_0 + m_1)}{r_1^3}\mathbf{r}_1 + \frac{Gm_2}{\Delta^3}\mathbf{\Delta} - \frac{Gm_2}{r_2^3}\mathbf{r}_2 \quad (1)$$

where \mathbf{r}_1 is the vector from m_0 to m_1 , \mathbf{r}_2 is the vector from m_0 to m_2 , Δ is the vector from m_1 to m_2 , and $\dot{x} = dx/dt$ etc.

Resolving the acceleration on m_1 into components in the radial and tangential directions, and noting that the radial and tangential accelerations can be expressed as $\ddot{r}_1 - r_1(\dot{\theta}_1)^2$ and $r_1\ddot{\theta}_1 + 2\dot{r}_1\dot{\theta}_1$ respectively, we get

$$\begin{aligned}\ddot{r}_1 - r_1(\dot{\theta}_1)^2 &= -G \left[\frac{(m_0 + m_1)}{r_1^3} + \frac{m_2}{\Delta^3} \right] r_1 + Gm_2 \left[\frac{1}{\Delta^3} - \frac{1}{r_2^3} \right] r_2 \cos(\theta_1 - \theta_2) \\ r_1\ddot{\theta}_1 + 2\dot{r}_1\dot{\theta}_1 &= -Gm_2 \left[\frac{1}{\Delta^3} - \frac{1}{r_2^3} \right] r_2 \sin(\theta_1 - \theta_2)\end{aligned}\quad (2)$$

where (r_1, θ_1) are the polar coordinates of body m_1 with respect to m_0 . The acceleration components for body m_2 have a similar form to those for m_1 .

We now consider a configuration in which the 3 bodies lie at the corners of an equilateral triangle of side a , with all the masses revolving on circular orbits about the centre of mass with angular speed n . In this case $r_i = \Delta = a$, $\dot{r}_i = \ddot{r}_i = \ddot{\theta}_i = 0$ and $\dot{\theta}_i = n$ for $i = 1, 2$, and Eqns. 2 are satisfied provided that $n^2 a^3 = Gm_{\text{tot}}$, where m_{tot} is the sum of all the masses. Hence, an equilateral triangle configuration is an equilibrium point in the general 3-body problem as well as in the restricted problem.

To examine the stability of configurations close to the equilibrium point, we expand Eqns. 2 in terms of r_i and θ_i , being careful not to make any assumptions about the relative sizes of the masses at this stage. In expanding the equations, we define 2 new variables $\theta = \theta_1 - \theta_2$ and $s = (r_1 - r_2)/a$, and we consider small deviations from the equilibrium configuration corresponding to $\theta = \pi/3$ radians and $s = 0$. The expanded equations for m_1 are

$$\ddot{r}_1 - 2an(\dot{\theta}_1 - n) - n^2 r_1 = -\frac{Gm_{\text{tot}}}{a^2} \left(3 - \frac{2r_1}{a} \right)$$

$$\begin{aligned}
 & - \frac{Gm_2}{a^2} \left[B(\theta)(1 - \cos \theta) + \frac{3s}{2}(1 + \cos \theta) \right] \\
 a\ddot{\theta}_1 + 2n\dot{r}_1 &= - \frac{Gm_2 \sin \theta}{a^2} \left[B(\theta) - \frac{3s}{2} \right]
 \end{aligned} \tag{3}$$

where

$$B(\theta) = \left[\frac{1}{2 \sin(\theta/2)} \right]^3 - 1 = -\frac{3\sqrt{3}}{2} \left(\theta - \frac{\pi}{3} \right) + \dots \tag{4}$$

The equations for m_2 are similar except that $\sin \theta$ is replaced with $-\sin \theta$ and s is replaced by $-s$. In Eqn. 3, we have neglected terms proportional to $sB(\theta)$. These terms are negligible for orbits very close to the equilibrium point.

We can obtain a single pair of equations by taking the difference of the radial equations for m_1 and m_2 , and also the difference of the tangential equations. Introducing a new variable $\alpha = \theta - \pi/3$, and retaining only the linear term in the expansion for $B(\alpha)$, we get

$$\begin{aligned}
 \ddot{s} - 2n\dot{\alpha} + \Gamma n^2 \alpha - (3 - K)n^2 s &= 0 \\
 \ddot{\alpha} + 2n\dot{s} - n^2 K \alpha + \Gamma n^2 s &= 0
 \end{aligned} \tag{5}$$

where K and Γ are constants that depend only on the masses:

$$\begin{aligned}
 K &= \frac{9(m_1 + m_2)}{4m_{\text{tot}}} \\
 \Gamma &= \frac{3\sqrt{3}(m_1 - m_2)}{4m_{\text{tot}}}
 \end{aligned} \tag{6}$$

Following Murray and Dermott (1999), the general solution to Eqn. 5 is $\alpha = \sum_{j=1}^4 \alpha_j \exp(\lambda t)$ and $s = \sum_{j=1}^4 s_j \exp(\lambda t)$, where the α_j and s_j are constants. The frequencies λ are found by solving the determinant of the 4 first-order equations equivalent to the two second-order equations in Eqns. 5. This gives the condition

$$(\lambda/n)^4 + (\lambda/n)^2 + [3K - K^2 - \Gamma^2] = 0 \tag{7}$$

When the 3 bodies are slightly displaced from equilibrium, they will undergo small oscillations about this point provided that all of the frequencies are purely imaginary, and

this requires that

$$1 \geq 4(3K - K^2 - \Gamma^2) \geq 0 \quad (8)$$

For the restricted case, where $m_2 = 0$, we recover the standard condition for stability that

$$\frac{m_1}{m_{\text{tot}}} \leq \frac{9 - \sqrt{69}}{18} = 0.03852 \dots \quad (9)$$

For the case of equal-mass secondaries, where $m_2 = m_1$, we find that the sum of their masses must be slightly less than the maximum mass for the restricted case:

$$\frac{m_1 + m_2}{m_{\text{tot}}} \leq \frac{6 - 4\sqrt{2}}{9} = 0.03812 \dots \quad (10)$$

It is straightforward to show that the critical value of $(m_1 + m_2)/m_{\text{tot}}$ always lies between these 2 values when $0 < m_2 < m_1$. (After submitting the original version of this manuscript, Michael Nauenberg informed us that Siegler and Moser (1971) derived an equivalent expression for the existence of periodic orbits in the general 3-body problem).

For the range of masses in which the equilibrium points are stable, K and Γ are small quantities, and we can derive approximate expressions for the oscillations periods P , which are related to the frequencies by $P = 2\pi/|\lambda|$. The periods are given by

$$\begin{aligned} P_1 &\sim P_{\text{Kep}} \left[1 + \frac{27(m_1 + m_2)}{8m_{\text{tot}}} \right] \\ P_2 &\sim P_{\text{Kep}} \sqrt{\frac{4m_{\text{tot}}}{27(m_1 + m_2)}} \end{aligned} \quad (11)$$

where $P_{\text{Kep}} = 2\pi/n$ is the orbital period. The first of these is clearly close to the orbital period, while the second represents the period of librations in θ about the equilibrium point. For a pair of planets with masses comparable to Jupiter or Saturn orbiting a solar-mass star, the libration period is roughly an order of magnitude larger than the orbital period.

Figure 1 shows two examples of the behavior of equal-mass planets with $m_1 = m_2 = 0.25M_{\text{JUP}}$ which are orbiting a solar mass central star and participating in co-planar

co-orbital librations. In each case, the osculating initial eccentricities and arguments of periastron are given by $e_1 = e_2 = 0.01$, and $\varpi_1 = \varpi_2 = 0.0$. Planet 1 is started at periastron passage, and Planet 2 is started 60 days ahead of periastron passage. The motion is plotted in the co-rotating frame over a 50 year timespan. The first orbit has initial osculating periods $P_1 = 365\text{d}$, and $P_2 = 355\text{d}$. In this case, the planets exhibit Tadpole-like librations about the equilateral configuration. The second orbit has a more discrepant pair of initial osculating periods, with $P_1 = 370\text{d}$ and $P_2 = 350\text{d}$. In this case, the larger initial perturbation from equilateral equilibrium causes the planets to execute horseshoe-like librations, and the motion is symmetric about a 180° separation. For both orbits, there is no visible alteration in behavior over a 10 million year trial integration.

We note that the Saturnian satellites Janus and Epimetheus provide a solar system example of a horseshoe-type 1:1 resonance. Janus and Epimetheus have a mass ratio $M_J/M_E \sim 0.25$. Their combined mass is tiny in comparison to Saturn, however, $\mu = 4.6 \times 10^{-9}$ (Yoder, Synnott, & Salo 1989).

Figure 2 shows a series of surfaces of section in which the difference in osculating semi-major axis ($a_2 - a_1$) is plotted against the longitudinal separation of the planets every time planet 1 reaches periastron. For initial period differences $P_1 - P_2 < 20\text{d}$, as with the first example orbit shown in Figure 1, the orbits are of the tadpole-type. A separatrix near $P_1 - P_2 = 20\text{d}$ shows that there is a transition to horseshoe type orbits at larger initial period separations. For the assumed initial conditions, the last stable horseshoe orbit occurs when $P_1 - P_2 = 27\text{d}$. Beyond this initial period separation, the twice-per-libration close encounters between the planets impart momentum kicks that are large enough to disrupt the resonant relationship. As the planet masses are increased, the width of the stable horseshoe region in ΔP decreases. When the planets reach $M_1 = M_2 = 0.4M_{\text{JUP}}$, a set of numerical integrations shows that the region of stable horseshoe orbits has disappeared. One can thus

hope to find pairs of Saturn-mass planets executing horseshoe orbits around a solar mass star ($M_{\text{SAT}}/M_{\odot} \sim 0.0003$, but one will not find two Jupiter-mass planets participating in this configuration ($M_{\text{JUP}}/M_{\odot} \sim 0.001$). Work is under way (Novak, Laughlin & Chambers 2002) which will further delineate the various stability boundaries for 1:1 configurations.

We point out that the surfaces of section corresponding to the motion of equal-mass planets (Figure 2) produce slightly fuzzy curves which are not clearly bounded. The finite width of these sections indicates that there is no isolating integral constraining the motion. In the planar restricted three-body problem, such an integral (the Jacobi constant, C_J), does exist, and the analogous curves in the surface of section have sharp boundaries. In this case, however, the motion of the planets is not restricted, and over extremely long periods, the system should be able to diffuse out of the resonant configuration, unless the orbits are strictly periodic.

Figure 3 shows the radial velocity component of the central star along a line of sight which views the two systems of Figure 1 in an edge-on configuration. The time baseline is 15 years. Over this period, the planets undergo a significant fraction of a libration. The resonant motion is visible in the stellar reflex velocity as an envelope modulating the high frequency sinusoid corresponding to the fundamental orbital frequency of the system. When the planets have a large angular separation, their contributions to the radial velocity of the star tend to cancel out. Furthermore, the envelope modulation, with its characteristic accordion-like shape is dictated by the masses of the planets, and if a system is found in the 1:1 resonance, it will not be subject to the $\sin i$ degeneracy that pertains to Keplerian fits.

Figure 4 shows a fundamentally different 1:1 resonance that may exist in extrasolar planetary systems. In this rather exotic configuration, one planet begins with a high eccentricity orbit, while the other traces a lower eccentricity orbit. We refer to this state of affairs as a 1:1 “eccentric resonance”. The configuration shown has equal-mass $1 M_{\text{JUP}}$

planets, on orbits with initial periods of $P_1 = P_2 = 360\text{d}$. The planets initially avoid close encounters by maintaining relatively small differences in longitude during pericenter passage of the eccentric member of the pair. In the situation shown in Figure 4, at the moment of periastron passage of the eccentric planet, the low eccentricity planet has already passed periapse, and has a mean anomaly $M = 40^\circ$. The planet-planet perturbations are most effective when the eccentric planet is near aphelion. During this period, which is marked by solid lines on the orbital curves, the planet on the near-circular orbit transfers angular momentum to the eccentric planet. As shown in Figure 5, this angular momentum transfer leads to a periodic exchange of eccentricities between the planets over a ~ 800 year secular cycle. (Heavier planets experience shorter secular cycles.) Both planets experience only small amplitude high-frequency oscillations in osculating semi-major axis during the secular cycle, indicating that the resonant lock is mediated by angular momentum rather than energy exchange. For $\mu = 0.001$, the resonant lock between the two planets is very stable, and is maintained with no outward variation over the course of a ten million year test integration. Numerical experiments show that the resonance breaks down for values $\mu \sim 0.035$.

As was the case with the tadpole and horseshoe type 1:1 resonances, the line-of-sight radial velocity variation of the central star shows a distinctive pattern, and is plotted over the initial ten year span in Figure 6. Each periastron passage of the eccentric planet is marked by a steep decrease in the radial velocity. Within a radial velocity data set, the presence of an eccentric 1:1 resonance might typically be indicated by a single highly errant velocity measurement superimposed on an otherwise sinusoidal pattern.

We note that because the 1:1 resonance is the lowest-order resonance, the effect of planet-planet perturbations are seen most dramatically in a radial velocity data set of given precision. Indeed, it may be the case that such systems are currently sitting unrecognized

within the accumulated data of the ongoing radial velocity surveys.

3. Orbital fitting of 1:1 resonant systems

As discussed above, and shown in Figures 3 and 6, a pair of extrasolar planets participating in the 1:1 resonance produces a readily detectable radial velocity signature. Because the 1:1 resonance involves strong planet-planet interactions, however, the usual procedure of testing Keplerian planetary orbits to minimize the χ^2 of the orbital fit will not give correct results.

The discovery of the 2:1 resonance between GJ 876 b and c has shown that planet-planet dynamical effects provide a crucial descriptive ingredient of a particular system (Laughlin & Chambers, 2001; Rivera & Lissauer, 2001; Nauenberg, 2002). In this section we describe the application of a straightforward self-consistent dynamical fitting procedure which can uncover a 1:1 resonant configuration within a set of radial velocities.

In order to illustrate the fitting procedure, we have adopted the latest Keck Telescope radial velocity data set for GJ 876 (Marcy et al 2001; Marcy, personal communication). This data set includes 63 radial velocity measurements spanning 1532 days. Each velocity has an associated measurement uncertainty which is estimated from the internal cross correlation of the lines within the spectra. These velocity uncertainties range from 2.8 m/s to 8.3 m/s, and their r.m.s. value is 5.14 m/s. In Table 1, we have specified the osculating orbital elements of a hypothetical tadpole-type resonant pair orbiting a solar-mass star. Using these orbital elements at the epoch of the first radial velocity point as initial conditions, we integrated the hypothetical system forward in time for the duration spanned by the actual radial velocity observations of GJ 876. We then sampled the radial velocity of the parent star in response to the hypothetical 1:1 resonant pair at the 63 observational epochs.

For each point, we then added radial velocity noise drawn from a Gaussian distribution of half-width given by the actual quoted velocity errors. This yields a synthetic radial velocity data set from which we can attempt to reconstruct the orbital parameters of the planets.

The top panel of Figure 7 shows the power spectrum of the synthetic radial velocity data set. There is a single significant peak at the fundamental 30 day period, and the spectrum gives little indication of the presence of two planets in the data. In particular, the accordeon-like modulation of the radial velocity curve due to the 300 day libration frequency between the planets is not immediately apparent in the power spectrum, as can be seen by comparing with the power spectrum produced by a single planet of $K = 75\text{m/s}$ on a circular 30 day orbit (bottom panel of Figure 7). In both cases, the power spectrum shows only a single significant peak.

In order to fit the synthetic 1:1 resonant system, we have employed a two-stage method. In the first stage, we use a genetic algorithm (Goldberg, 1989) as implemented in Fortran by Carroll (1999) for public domain use. The genetic algorithm starts with an aggregate of osculating orbital elements, each referenced to the epoch of the first radial velocity observation ($T_0 = 2450602.0931$). Each set of elements (genomes) describes a unique three-body integration and an associated radial velocity curve for the central star. The fitness of a particular genome is measured by the χ^2 value of its fit to the radial velocity data set. At each generation, the genetic algorithm evaluates the χ^2 fit resulting from each parameter set, and cross breeds the best members of the population to produce a new generation.

Because the fundamental 30 day period of the system is clearly visible in the power spectrum, the genetic algorithm is constrained to search for 1:1 resonant configurations in which the initial period ranges for the planets are $29\text{d} < P_1 < 31\text{d}$, and $29\text{d} < P_2 < 31\text{d}$. The initial arguments of periaapse and mean anomalies of the two planets are allowed to

vary within the allowed 2π range. The radial velocity half-amplitudes of the planets are required to fall in the range $0 < K_1 < 150\text{m/sec}$ and $0 < K_2 < 150\text{m/sec}$. The planetary eccentricities are allowed to vary within the full $0 < e < 1$ range.

With these very liberal constraints on the space of osculating initial orbital elements, the Genetic Algorithm rapidly identifies a set of parameters having $\chi = 1.27$. This tentative fit is then further improved by use of Levenberg Marquardt minimization (Press et al. 1992) to produce a fit to the data having $\chi = 0.97$. This fit is shown in Figure 8, and in the third and fourth columns of Table 1. The excellent agreement between the input system and the fitted solution shows that a 1:1 resonant pair is readily identifiable if it exists within a radial velocity data set comparable to the GJ 876 velocities. As the radial velocity surveys continue, an increasing number of target stars will have velocity data sets of this quality.

4. The Formation and Migration of Trojan Planets

The foregoing sections show that 1:1 resonant configurations are viable from an orbital stability standpoint, and are also readily detectable should they exist. The natural question, therefore, is: Can co-orbital planets form? We believe that the answer is yes, and in a forthcoming work, we will present a detailed argument in favor of this hypothesis (Novak, Laughlin, & Chambers 2002). Here, we briefly outline our arguments.

The parameter space available to the eccentric 1:1 resonance and its close relatives has not yet been mapped in detail, but initial numerical surveys show that it is surprisingly large. A vast range of co-orbital configurations exist which are both stable and which roughly resemble the intermediate panels of Figure 5. It is challenging to imagine how such systems might form, but one scenario is as follows: A planetary system forms in which there are three major planets. The *v* Andromedae system provides a rough example (Butler et al

1999). A dynamical instability or collision then occurs between two of the planets, leaving two survivors participating in some form of the eccentric 1:1 resonance. We would expect that such dynamical formation channels are unlikely, but the cross section for this class of events could be calculated numerically in the event that a system of this type is discovered (Laughlin & Adams 1998, Ford, Rasio, & Havlikova 2001).

We expect that Tadpole or Horseshoe-type planetary pairs are more common, and that their formation is mediated by interaction with a protostellar disk. One possibility is that a pair of planets can form directly in a near equilateral configuration. Figure 9 shows a detail of a hydrodynamical calculation which was performed and discussed by Laughlin, Chambers and Fisher (2002). In this scenario, a planet with mass $0.75M_{\text{JUP}}$ is present within a protoplanetary accretion disk. The viscosity parameter of the disk in the region near the planet is of order $\alpha \sim 0.02$, and the planet, with its sub-Jovian mass, is only marginally capable of maintaining a gap in the disk. Material is seen to linger in the vicinity of the L_4 and L_5 points. The vortical flow pattern in these regions might lead to particle trapping and the accumulation of a second significant core (e.g. Adams & Watkins 1995, Barge & Sommeria 1995, Godon & Livio 2000). Recent high-resolution numerical simulations by Balmforth & Korycansky (2001) have shown that the large-scale vortical flow enveloping the horseshoe region nucleates additional smaller vortices, which may spur further formation of planetary cores.

If two planets form from a disk in a 1:1 horseshoe or tadpole configuration, the resonant lock is maintained as the planets migrate inwards as a result of their interaction with the disk. This effect is shown in Figure 10, which shows the result of a three-body integration of a star and a resonant 1:1 tadpole type Jovian-mass planetary pair. A small azimuthal torque $a_\phi = -3.4 \times 10^{-5} \text{AU/yr}^2$ is applied to one of the planets. Despite this uneven application of torque, the planets remain coupled together in resonance, and migrate inwards together.

Resonant migration leads to secular eccentricity increase for planets on first or higher order mean motion resonances, and as noted by Lee & Peale (2002), this increase leads to difficulties in constructing a plausible formation scenario for the planets orbiting GJ 876. In the case of 1:1 resonant migration, however, angular momentum and energy loss from the planets occurs at a rate which prevents a secular increase in eccentricity. Once formed, a 1:1 resonant pair is capable of migrating to small semi-major axes.

In our upcoming paper, we will describe a sequence of events which we believe is the most likely channel for forming observable 1:1 configurations. Our scenario starts with a major collision between two multiple Earth-mass cores in a nascent planetary system. The collision leads to the formation of a binary core, in much the same fashion as a giant impact is believed to have formed the Earth-moon system. The cores retain their individuality, and accrete gas from the surrounding nebula, leading to the formation of a bound double planet. This double planet migrates inward to small orbital radii, at which point the separation of the planets exceeds the Hill Radius. At this point, the planets scatter onto a horseshoe-type orbit, which can be subsequently damped to a trojan configuration.

4.1. Acknowledgments

We would like to thank Debra Fischer, Doug Lin, Geoff Marcy, Michael Nauenberg, and Greg Novak for useful discussions. Stan Peale provided a very prompt and informative referee’s report. This material is based upon work supported by NASA under contract No. RTOP 344-37-22-12 issued through the Origins of Solar Systems Program, and by funds from the University of California, Santa Cruz. JEC acknowledges support from an NRC Postdoctoral Program and from the NASA Origins of Solar Systems Program.

REFERENCES

- Adams, F. C., & Watkins, R., 1995, ApJ, 451, 314
- Balmforth, N. J., & Korycansky, D. G. 2001, MNRAS, 326, 833
- Butler, R. P., Marcy, G. W., Williams, E., McCarthy, C., & Dosanji, P. 1996, PASP, 108, 500
- Carroll, D. L. 1999, Genetic Algorithm (GA) Driver
(<http://cuaerospace.com/carroll/ga.html>)
- Chiang, E. I., Tabachnik, S., & Tremaine, S. 2001, AJ, 122, 1607
- Godon, P., & Livio, L., 2000, ApJ, 537, 396
- Goldberg, D. E. 1989, *Genetic Algorithms in Search, Optimization and Machine Learning*
(Addison Wesley: Reading MA)
- Lagrange, J. 1867-1892, *Oeuvres* 14 Volumes (Gauthier-Villars: Paris)
- Lee, M. H., & Peale, S. J. 2002, ApJ, 567, 596
- Laughlin, G., & Adams, F. C. 1998, ApJ, 508, L171
- Laughlin, G., & Chambers, J. 2001, ApJ, 551, 109
- Laughlin, G., hambers, J., & Fischer, D. 2002, ApJ Submitted
- Marcy, G.W., Cochran, W.D. & Mayor, M. 2000, in *Protostars and Planets IV*, ed. V. Mannings, A. P. Boss & S. S. Russell (Tucson: University of Arizona Press), p.1285
- Marcy, G. W., Butler, R. P., Fischer, D., Vogt, S. S., Lissauer, J. J., & Rivera, E. J. 2001, ApJ, 556, 296

- Murray, C. D. & Dermott, S. F. 1999, *Solar System Dynamics* (Cambridge University Press, Cambridge)
- Nauenberg, M., 2002 ApJ, In Press.
- Nauenberg, M., 2002 Private Communication
- Novak, G., Laughlin, G., & Chambers, J. 2002, In Preparation
- Press, W. H., Teukolsky, S. A., Vetterling, W. T., & Flannery, B. P. 1992, *Numerical Recipes: The Art of Scientific Computing* (Cambridge Univ. Press: Cambridge)
- Rivera, E., & Lissauer, J. 2001, ApJ 530, 454
- Routh, E. J. 1898, *A Treatise on the Dynamics of a Particle with Numerous Examples* (Cambridge Univ. Press: Cambridge)
- Shoemaker, E. M., Shoemaker, E. S., & Wolfe, R. F. 1989, in *Asteroids II*, ed. R. P. Binzel, T. Gehrels, & M. S. Matthews (University of Arizona Press: Tucson)
- Siegler, C.L. & Moser, J.K. 1971, *Lectures in Celestial Mechanics* (Springer).
- Yoder, C. F., Synnott, S. P., & Salo, H. 1989, AJ, 98, 1875

Fig. 1.— Examples of trojan orbits and horseshoe orbits. A detailed plot is shown in the right panel. In each case, the mass of both planets is $1 M_{\text{JUP}}$. The solid line corresponds to the horseshoe-type orbit. The dotted line corresponds to the tadpole-type orbit.

Fig. 2.— Surface of section showing a_1/a_2 and the difference in longitude $D = (M_1 + \varpi_1) - (M_2 + \varpi_2) = \lambda_1 - \lambda_2$ for a pair of co-orbital planets every time planet 1 reaches periapse. The loci of points centered on $a_1/a_2 = 1.0$, $\lambda_1 - \lambda_2 = 1.0472$ are executing tadpole-type orbits. The outermost loci correspond to horseshoe-type orbits.

Fig. 3.— Synthetic radial velocity variations for the planetary systems shown in Figure 1. The solid line corresponds to the horseshoe-type orbit. The dotted line corresponds to the tadpole-type orbit.

Fig. 4.— Planet orbits in an example 1:1 eccentric resonance. The solid lines indicate portions of the respective orbits swept out in a single period of time corresponding to 15% of the orbital period.

Fig. 5.— Evolution of planet orbits in an example 1:1 eccentric resonance.

Fig. 6.— Synthetic radial velocity variations for a planetary system participating in the 1:1 eccentric resonance. The radial velocity curve corresponds to the situation near the first panel of Figure 5, where one planet is highly eccentric while the other is on a near-circular orbit.

Fig. 7.— Upper panel: Power spectrum corresponding to a synthetic radial velocity data set produced using the hypothetical planetary system shown in Table 1, sampled at the epochs and velocity precision of the GJ 876 Keck radial velocities. Lower Panel: Power spectrum corresponding to a single planet on a circular orbit with $K = 75\text{m/s}$, and $P = 30\text{d}$, also sampled at the epochs and velocity precision of the GJ 876 data set.

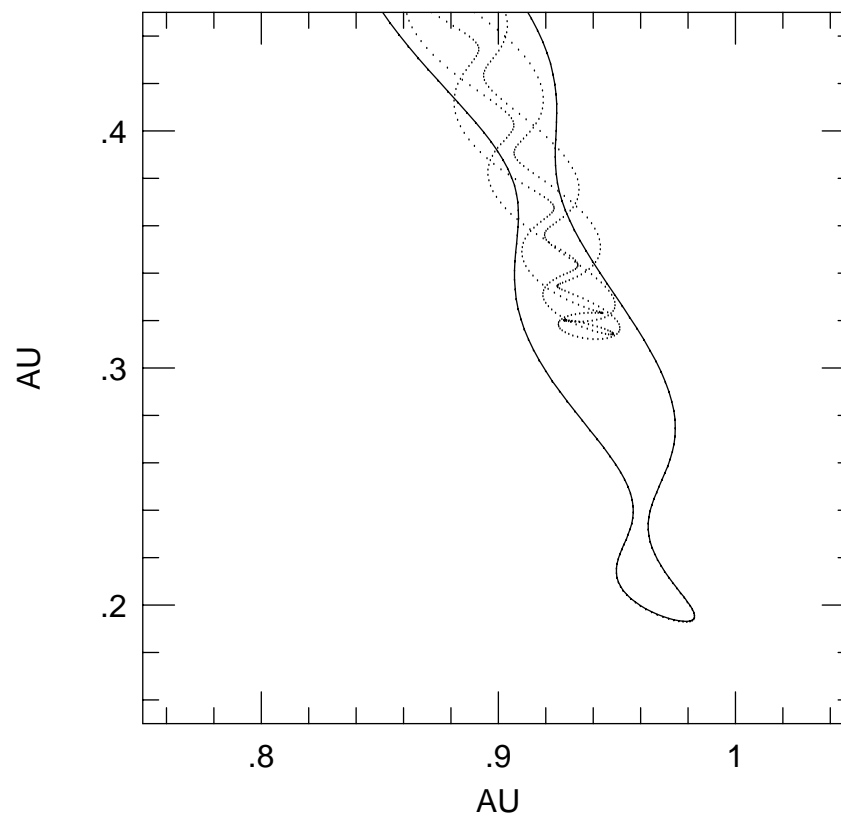
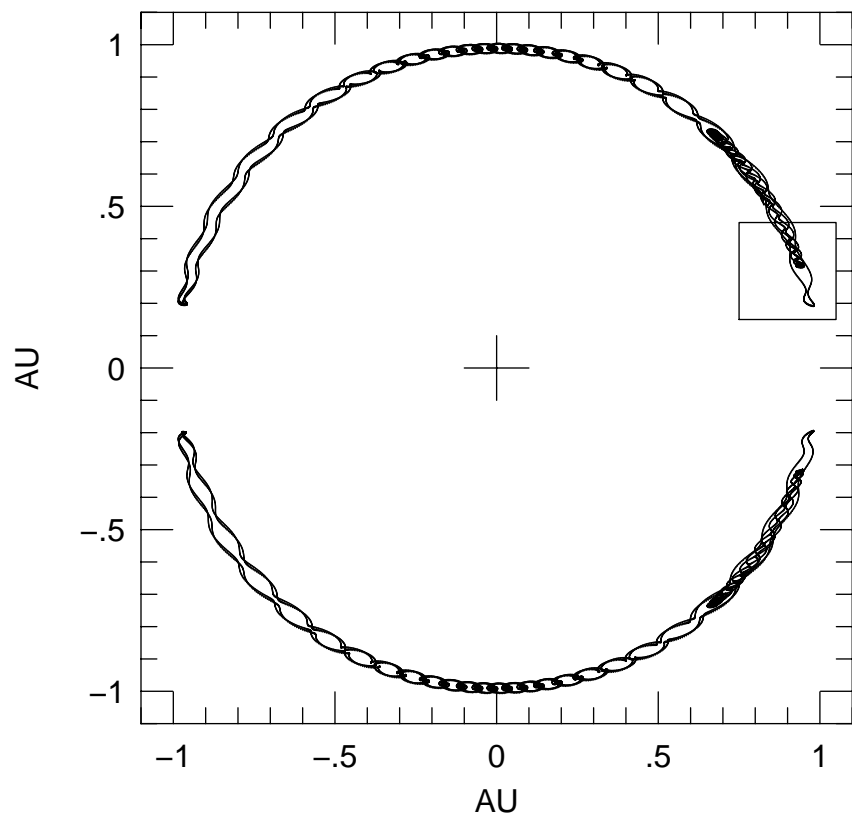
Fig. 8.— Synthetic radial velocity variations for the planetary system shown in Table 1 (solid line). The circular points with small vertical lines corresponding to errorbars represent a sample of the system with the properties of the GJ876 data set. A superimposed dotted line shows a fit to the sampled data obtained with a combined Genetic Algorithm and Levenberg-Marquardt procedure. It is hard to distinguish the difference between these two curves at the resolution of the plot.

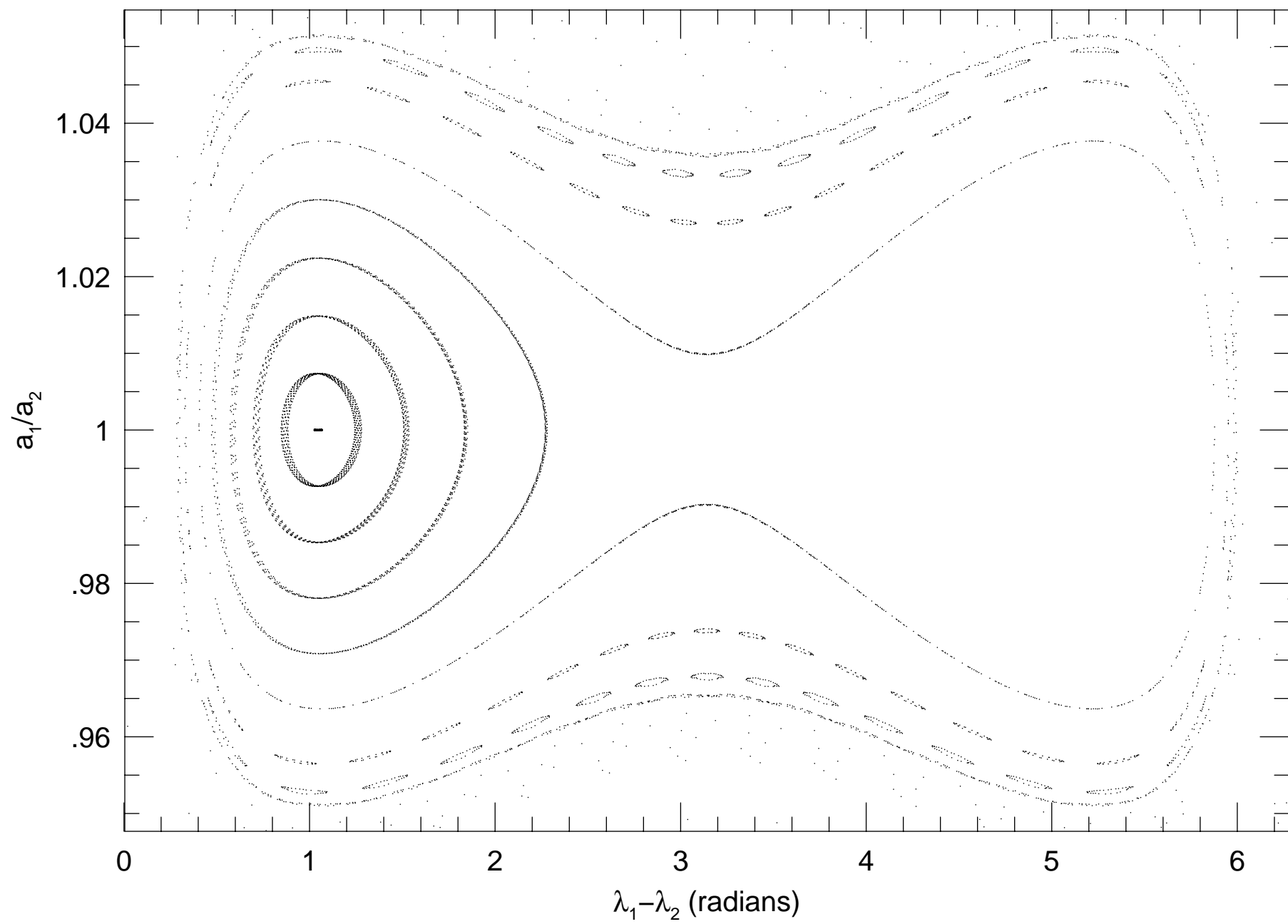
Fig. 9.— Detail of a hydrodynamical calculation of a planet clearing a gap in a disk. A vortical flow is observed around the L5 point. We hypothesize that such a vortex could trap particles and lead to the formation of a second planet trapped in 1:1 resonance with the first.

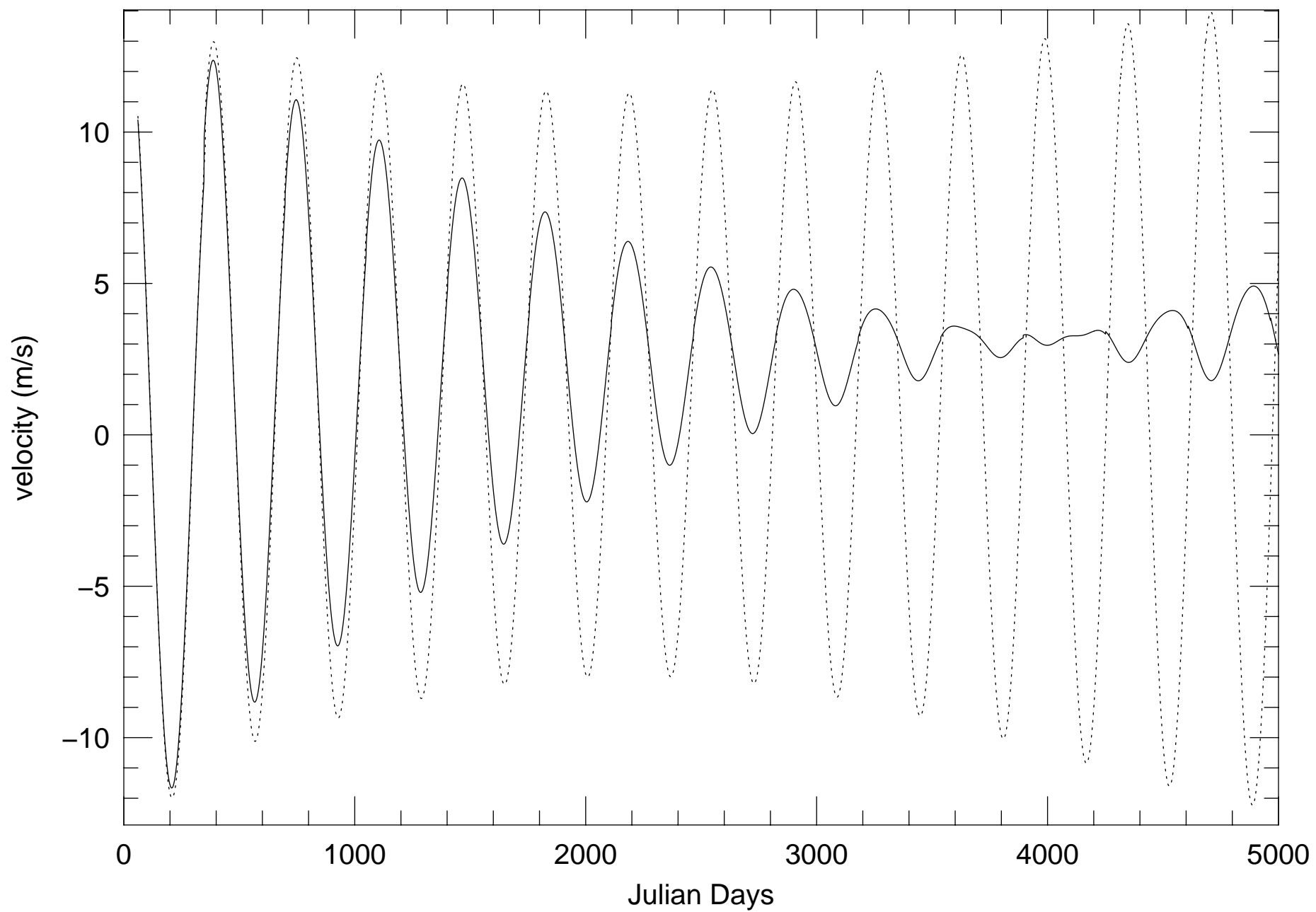
Fig. 10.— Evolution of a three-body simulation in which a pair of equal mass planets in 1:1 resonance migrate inward without showing secular increase in eccentricity. Torque is applied to only one of the planets. In the bottom panel, the eccentricities of both planets are shown, with planet b’s eccentricity plotted as dots, and planet c’s eccentricity plotted as a solid line.

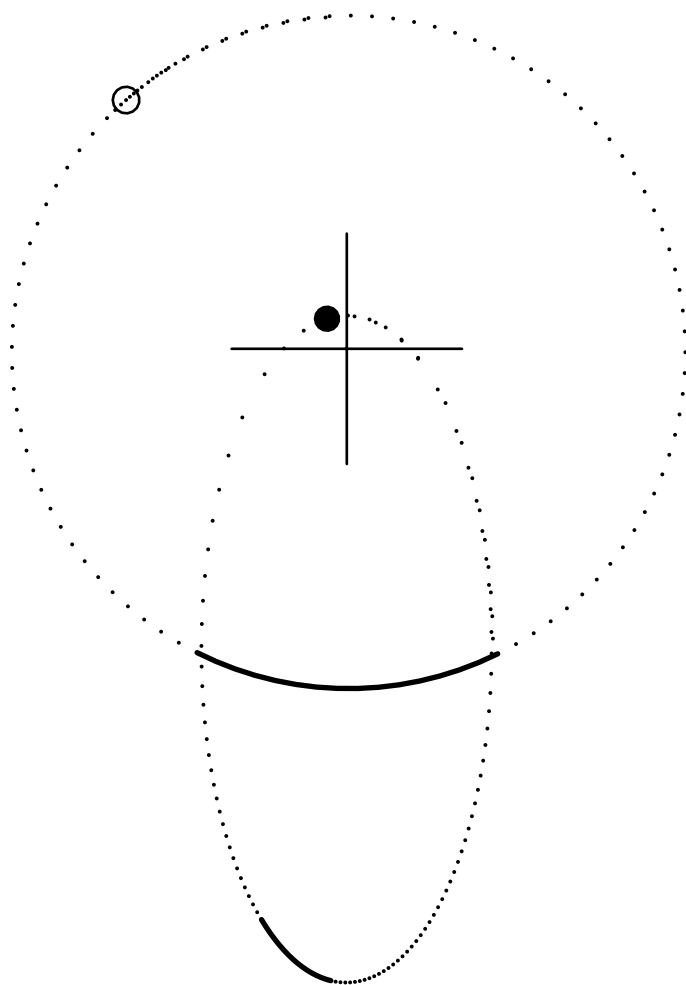
Parameter	Planet 1	Planet 2	Planet 1	Planet 2
	(Assumed Elements)		(Fitted Elements)	
Period (day)	30.000	30.000	29.919	30.037
K (ms^{-1})	50.000	100.00	49.233	99.694
Eccentricity	0.0500	0.0500	0.0418	0.0401
ω (deg)	180.00	180.00	195.02	174.29
Periastron Time (JD)	10.000	20.000	11.253	19.512

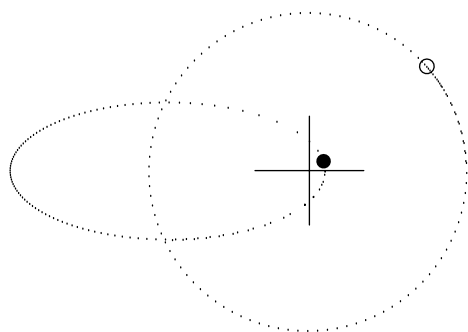
Table 1: **Assumed and Fitted Elements for 1:1 Resonant System (using GJ 876 data set)**



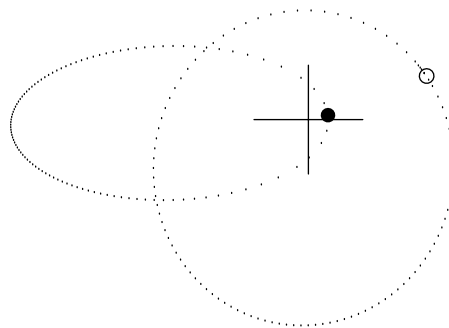




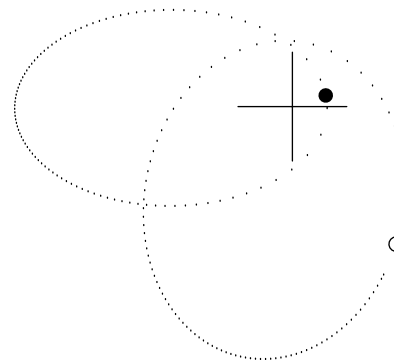




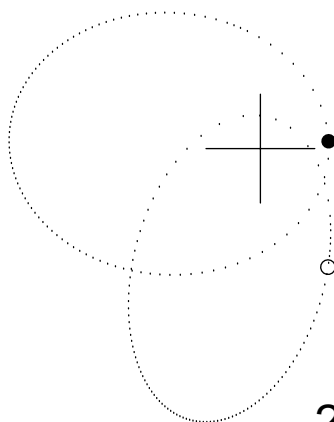
0 yr



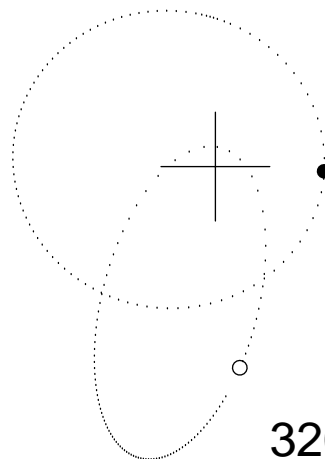
80 yr



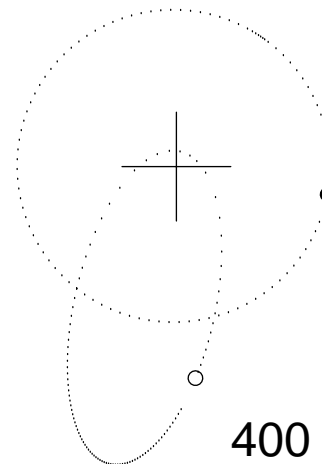
160 yr



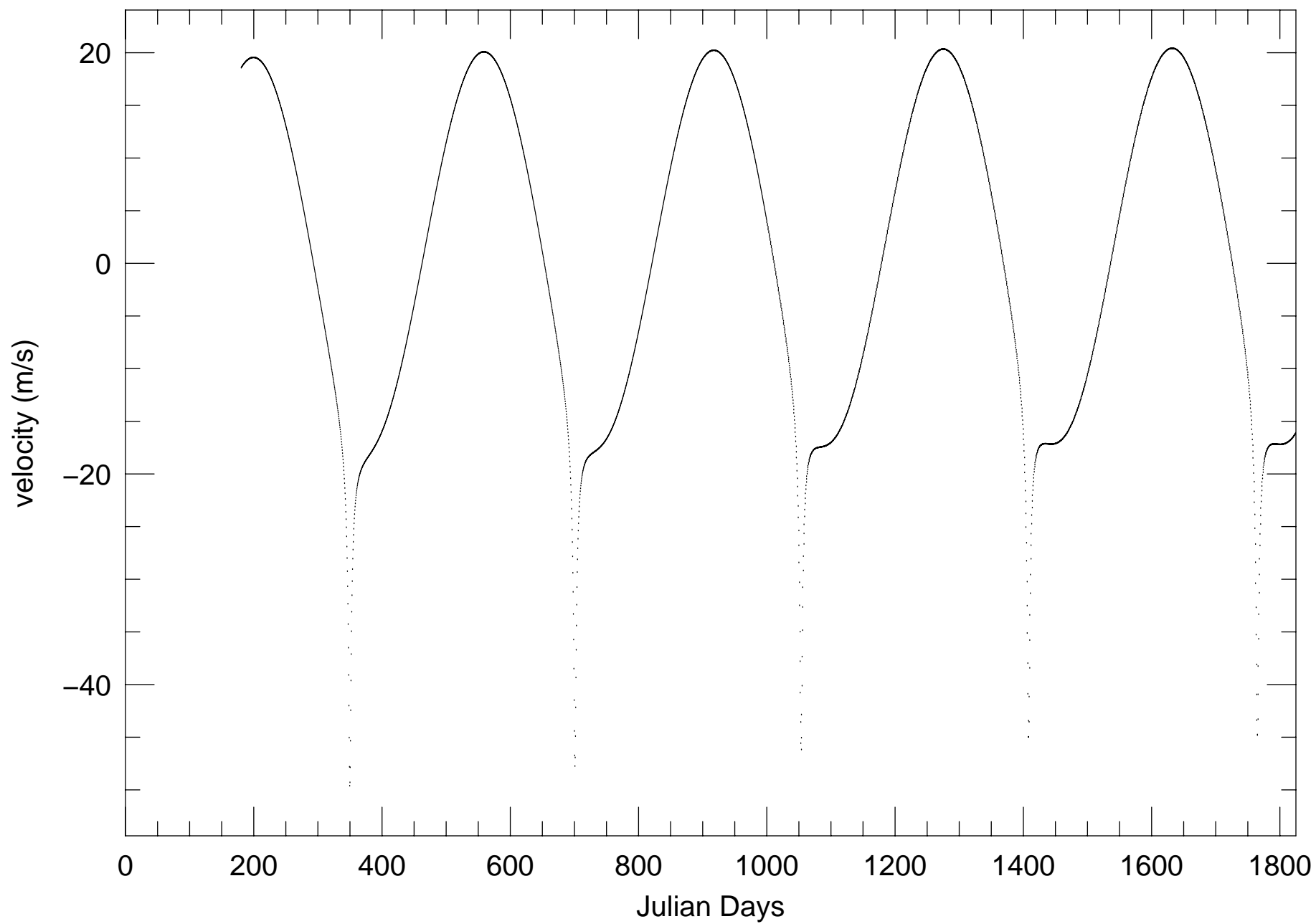
240 yr

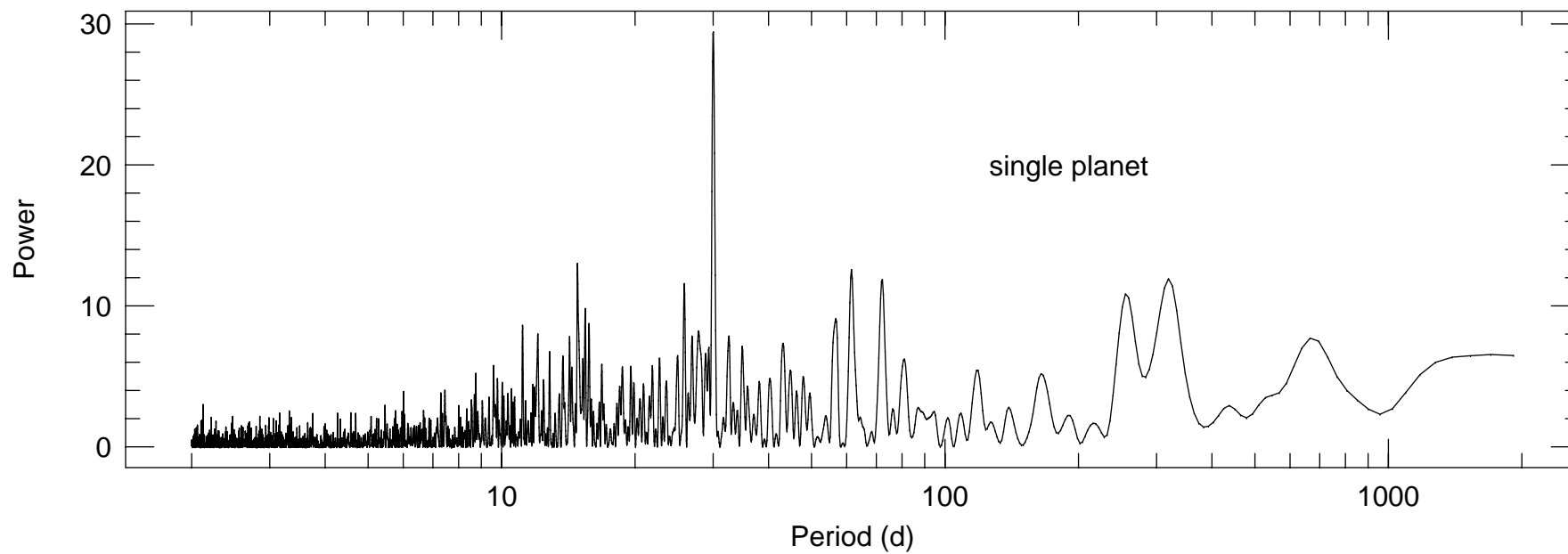
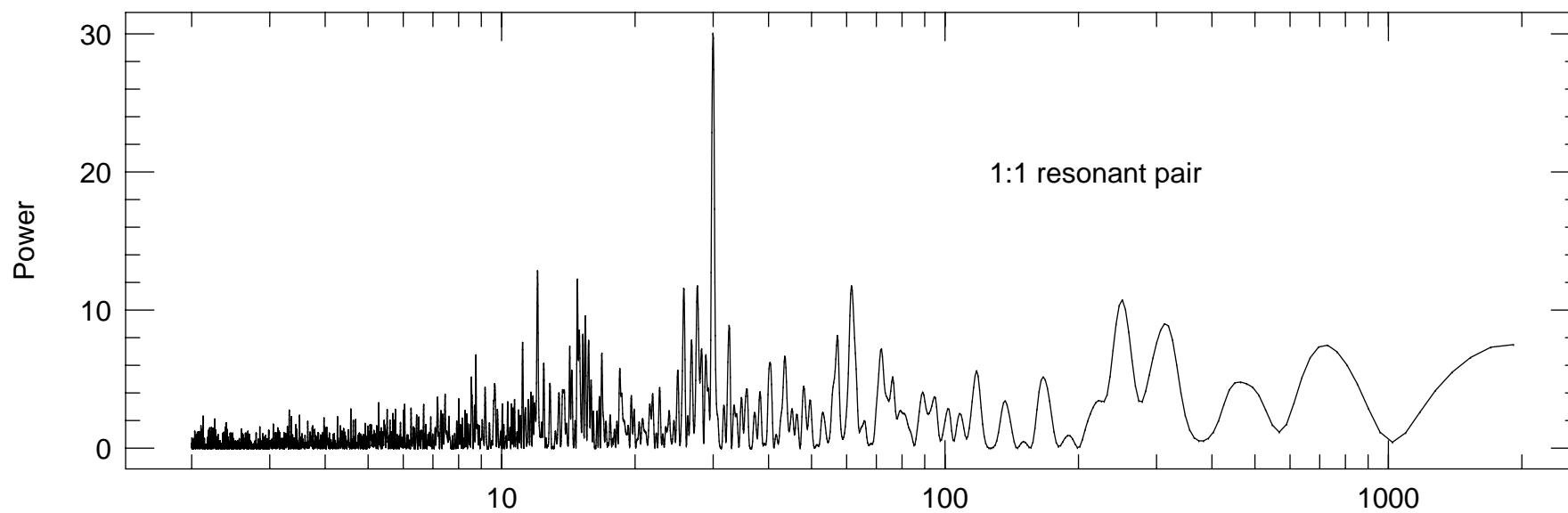


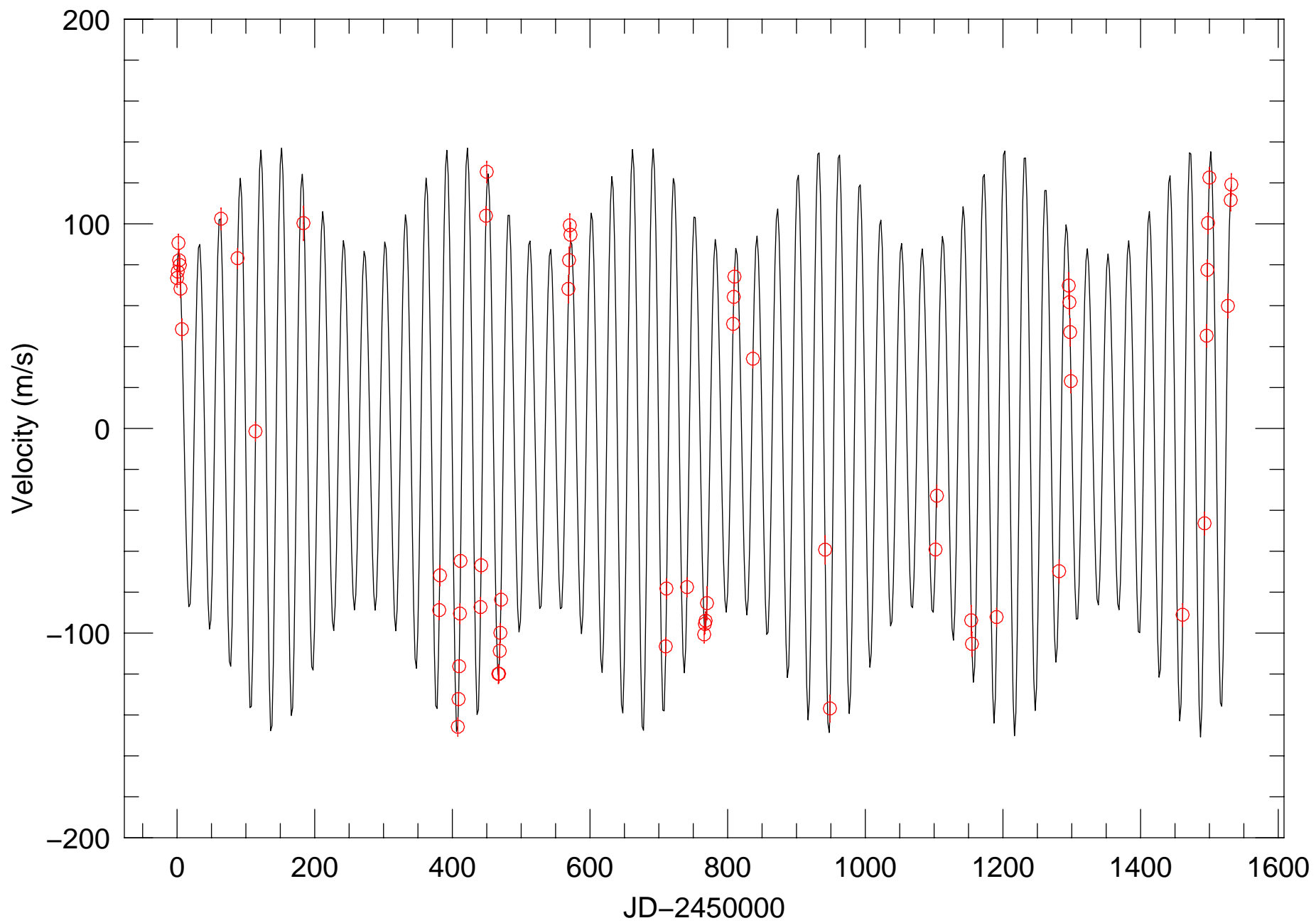
320 yr



400 yr







This figure "fig9.gif" is available in "gif" format from:

<http://arxiv.org/ps/astro-ph/0204091v1>

